Dose perturbations of unilateral Ti prosthesis in the dosimetry of 6 MV photon beam

Nicholas Ade and F.C.P. du Plessis

Medical Physics Department, University of the Free State, PO Box 339, Bloemfontein 9300, South Africa
E-mail: leroinicholson@yahoo.ca

Abstract. During irradiation of malignancies in the hip region with external megavoltage photon beams, the presence of metallic prostheses could partially shield the beam at the target and alter the dose distribution. This may cause a dramatic difference in treatment outcome. This study investigates the magnitude of 6 MV photon beam dose perturbations caused by unilateral titanium prosthesis and were measured with Gafchromic EBT2 film in a pelvic phantom made out of nylon slices. Dose perturbations were measured and compared using absorbed dose distributions for a range of field sizes between (3 × 3) and (10 × 10) cm^2. The magnitude of these perturbations was quantified as dose correction factors, DCFs which is defined as the ratio of the dose influenced by the prosthesis and the unaltered beam. A DCF of unity marks the margin between dose enhancement (where DCF > 1.0) and dose reduction (where DCF < 1.0). DCFs above unity were observed on the proximal (beam entry) side of the prosthesis while DCFs below unity occurred in the distal region (behind the prosthesis). For the studied field sizes maximum DCFs ranged between 1.22±0.02 and 1.23±0.02. Minimum DCFs ranged between 0.79±0.02 and 0.82±0.02. The DCFs on the proximal side of the prosthesis drop off rapidly with distance from the proximal nylon-prosthesis interface. The results of the study indicate that at the nylon-prosthesis interface, about 23% of dose enhancement is due to electron backscatter from the prosthesis and at least 18% of dose reduction behind the prosthesis is due to photon attenuation.

1. Introduction

A growing number of patients requiring external beam radiotherapy (EBRT) for malignancies in the pelvic region have metal implants such as hip prostheses [1]. The presence of metal implants during megavoltage photon radiotherapy could partially shield the beam at the target and alter the absorbed dose distribution [1-4]. This may cause a dramatic difference in treatment outcome [2]. It is believed that there is a decrease in tumour control due to a reduced target dose from beam attenuation by the prosthesis [3] or a rise in complication rates due to the local dose perturbations caused by implants [2]. The extent of dose perturbations is affected by factors such as the size, mass density, atomic composition and design of the prosthesis as well as beam energy. It is understood that the scientific understanding and approach of medical dosimetry for the presence of metal implants during EBRT is challenging [3-6]. Various implant materials include stainless steel, cobalt-chromium-molybdenum (Co-Cr-Mo) and titanium (Ti) [4-8]. The selection of an implant material is influenced by factors such as corrosion, fatigue resistance and mechanical strength [8]. Various experimental and Monte Carlo studies are available on photon beam dose perturbations of prostheses [1-11]. However, most of the

reports are limited to beam attenuation behind the prosthesis measured in water or plastic phantoms containing the prosthesis.

This study aims to investigate 6 MV photon beam dose perturbations of Ti prosthesis in front and behind the prosthesis using Gafchromic film measurements in a novel pelvic phantom. The newly designed phantom consists of a stack of nylon slices with a built-in unilateral Ti prosthesis.

2. Materials and methods

2.1. The novel pelvic phantom and film calibration

The phantom employed in this work is a locally fabricated pelvic phantom with an in-built Ti hip prosthesis and was designed for film dosimetry. Figure 1 shows the novel symmetrical phantom consisting of a stack of 25 Nylon 12 slices (each slice is 1.0±0.1 cm thick) of which some are fitted with Ti discs to form a unilateral Ti prosthesis. Nylon 12 is a polymer with formula $[(CH_2)_{11}CONH]_n$. The pelvic phantom contains bony structures including the spinal cord and pelvic bone constructed from tissue-equivalent substitutes. The components and material compositions (% by mass) of the tissue-equivalent substitutes include: Araldite GY-6010 epoxy resin (36.4), Jeffamine T-403 hardener (14.6); silicon dioxide (25.5) and calcium carbonate (23.5). The diameter of the Ti disc in the plane of measurement considered in this study is 2.7±0.1 cm. A thin layer of tissue material (nylon) located between the prosthesis and bone defines the bone-prosthesis interface.

All irradiation measurements reported in this study are from exposures of a single batch of Gafchromic® EBT2 films (Lot #: 01201501) in a 6 MV photon beam produced by a Philips SL75 linear accelerator. Before dose perturbation measurements, film calibrations were performed for conversion of optical density (OD) to dose in related approaches as reported in literature [13] using a rational calibration function of the type [14]:

$$X(D) = A + [B/(D - C)] \quad \textbf{(1)}$$

where $X(D)$ is the film response (OD) at dose D, and A, B and C are parameters that can be fitted to the calibration data using a least square optimization method. Calibration was performed by placing five 10 x 4 cm^2 film pieces horizontally (one at a time) inside a 30 x 30 cm^2 RW3 slab phantom at 10 cm depth on the central axis of a (10 x 10) cm^2 6 MV beam at 100 cm source-to-phantom surface distance. The film pieces were irradiated to dose values between 0 and 245 cGy. Irradiated films were digitized using an Epson Perfection V330 Photo flat-bed document scanner 24 hours post exposure to allow for polymerization.

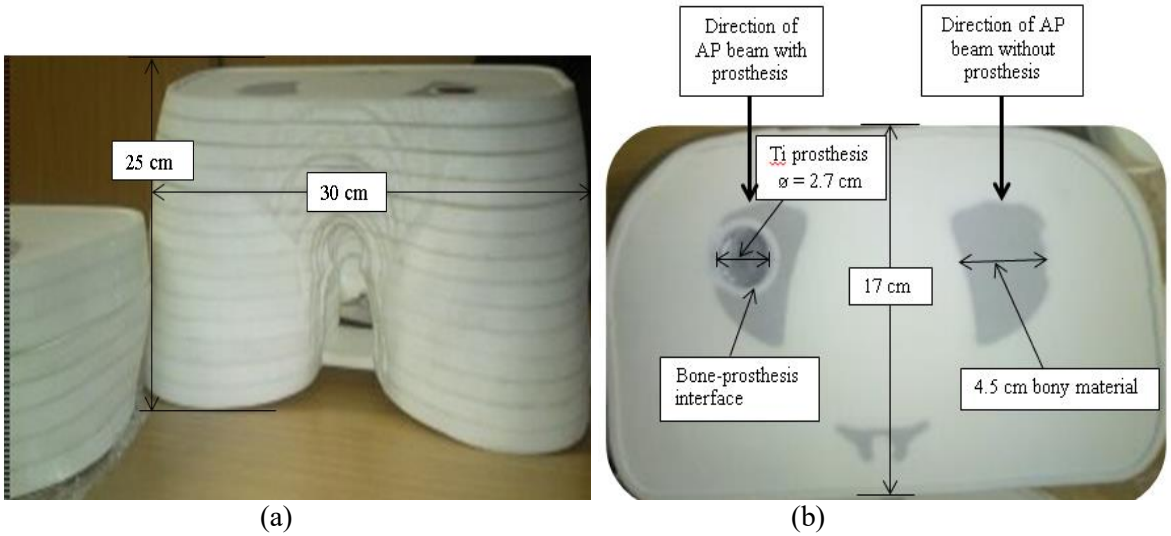

(a) (b)

Figure 1. Picture of novel pelvic phantom (a) showing unilateral Ti prosthesis in the measurement plane and the beam (anterior-posterior (AP)) directions incident on the phantom (b).

2.2. Dose perturbation measurements

Perturbations in absorbed dose distributions due to the presence and influence of the Ti prosthesis were measured and compared using dose maps and profiles for a range of field sizes. The pelvic phantom was placed in the supine position and dose distributions were acquired using single anterior-posterior (AP) (figure 1) beams for field sizes of (3 x 3), (5 x 5) and (10 x 10) cm^2. The measurements were acquired with and without the prosthesis by fitting cut EBT2 film pieces from a single batch (Lot #: 01201501) in the phantom. That is, as the phantom is symmetrical measurements were taken on the left side (with the prosthesis) and on the right side (without the prosthesis). Each fitted film piece covered only half (left or right side) of the measurement plane. Hence for the three field sizes studied, six pieces of film were used for the 6 MV beam and each film piece was irradiated separately. Employing a 100 cm source-to-axis distance (SAD) for each field size, an absorbed dose of 300 cGy was delivered at isocentre to each film fitted in the phantom at a depth of 8.5 cm from the surface to the centre of the phantom. The magnitude of dose perturbations caused by the prosthesis on measured dose distributions was quantified as dose correction factors, DCFs (enhancement and reduction) which is defined as the ratio of the dose influenced by the prosthesis and the unaltered beam.

3. Results and Discussion

3.1. Film calibration

Film images were digitized as raw 48-bit RGB (16 bits per colour) and saved as tagged-image-file format (TIFF) image files in a related approach as reported elsewhere [13]. Digitized images were then processed employing the 16 bits red channel of the scanned RGB images. Calibration curves for the red channel are shown in figure 2 with points corresponding to the measured mean OD at the corresponding dose. Superimposed on these points is the fitted rational function (1) with fitting coefficients of A = 0.794, B = -149.260 and C = -255.068.

3.2. Dose distribution measurements

Figures 3(a) – (e) show 6 MV photon beam dose distributions measured with Gafchromic EBT2 films in the pelvic prosthesis phantom for a (10 × 10) cm^2 field. In these figures the dose maps measured with (figure 3(a)) and without (figure 3(b)) the prosthesis, are displayed. The incident beam direction on the phantom for each dose image is indicated in figure 3(a). The colour palette (figure 3(c)) shows the dose variation on the maps. The profiles for the dose maps displayed in figures 3(a) and (b), just before the beam enters the prosthesis (proximal side) and just after it exits the prosthesis (distal side) are presented in figures 3(d) and (e), respectively. The horizontal lines drawn through the dose images show where the profiles were extracted. It could be observed on the dose maps and profiles that the dose increases at the nylon-prosthesis interface on the proximal side and decreases (attenuates) in the distal region of the prosthesis. The dose escalation is due to electron backscatter from the prosthesis and the dose decrease is due to beam attenuation just after the beam exits the prosthesis [15]. The dose increase depicted by the peak and attenuation depicted by the dip in figures 3(d) and (e) (red curves) are indicated by the purple bands, respectively. The dip indicated by light blue band in figure 3(d) shows beam attenuation by bone for the case of no prosthesis (dark blue curve). The dose increase and attenuation were also observed for the (5x5) cm^2 and (3x3) cm^2 images and profiles.

Figures 4(a) and (b) show 6 MV depth dose curves for (5 x 5) cm^2 and (3 x 3) cm^2 fields, respectively obtained from the dose maps. Regions consisting of nylon (white), bone (blue), and prosthesis (purple) as indicated in these figures show where the photon beam pass through when directed on the phantom. Shown on figures 3(a) and (b) for the (10 x 10) cm^2 field are areas (vertical lines drawn through the images) where the depth dose curves were extracted. The influence of the prosthesis on the depth dose curves are noticeable as its presence causes significant dose modification (red lines) compared to the case with no prosthesis (blue lines). Similar to the observation made in figures 3(d) and (e), figures 4(a) and (b) show that there is dose enhancement on the proximal side of the prosthesis and dose reduction in the distal region when compared to the case with no prosthesis.

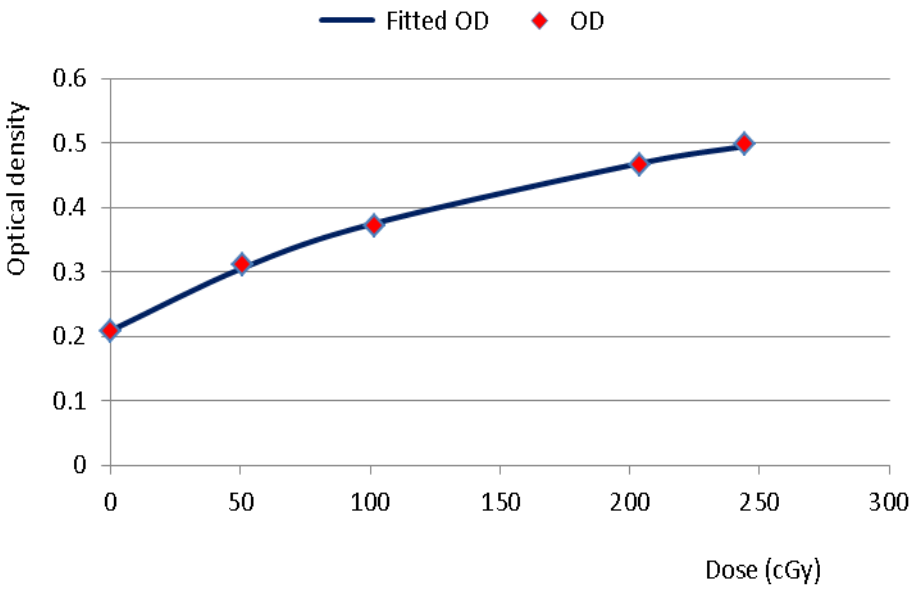

Figure 2. Red channel calibration curves for Gafchromic EBT2 film

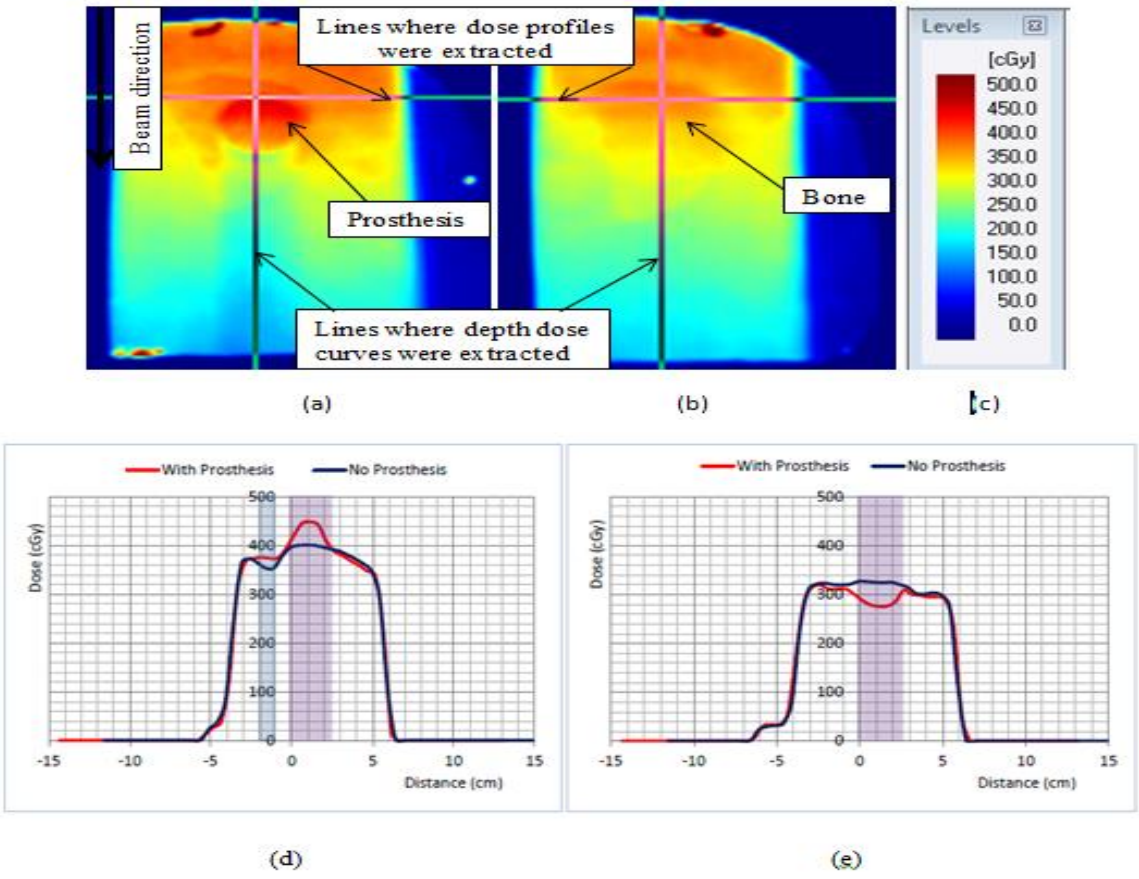

Figure 3. 6 MV dose distributions measured with EBT2 film for a (10 x 10) cm^2 field. The figure shows a comparison of dose maps with (a) and without (b) prosthesis on dose variation shown by the colour palette (c), and dose profiles on the beam entry (d) and exit (e) sides of the prosthesis.

3.3. Quantification of dose perturbation measurements

The extent of dose perturbations observed on the proximal and distal sides of the Ti prosthesis was quantified as dose correction factors DCFs (defined in section 2.2), calculated along the depth dose curves shown by the green lines in figures 4(a) and (b). A DCF of unity marks the margin between dose enhancement (where DCF > 1.0) and dose reduction (where DCF < 1.0) so figures 4(a) and (b) show that DCFs > 1.0 occur inside the prosthesis and on its proximal side while DCFs < 1.0 occur on the distal side of the prosthesis, primarily due to beam attenuation by the prosthesis.

For the studied 6 MV beam, maximum DCFs of 1.23±0.02, 1.22±0.02 and 1.22±0.02 (i.e., dose enhancements of 23±2%, 22±2% and 22±2%) which usually occurred on the beam entry side of the implant in the phantom (excluding the implant) were computed for (3 × 3), (5 × 5) and (10 × 10) cm^2 fields, respectively. Similarly, minimum DCFs of 0.82±0.02, 0.79±0.02 and 0.81±0.02 (i.e. dose reductions of 18±2%, 21±2% and 19±2%) which typically occurred on the beam exit side of the implant were obtained for (3 × 3), (5 × 5) and (10 × 10) cm^2 fields, respectively. The values quoted for the maximum and minimum DCFs for each field size are the averages of at least the six largest or lowest values and the errors are the standard deviations of the average values. The implant also receives a higher dose from the photon beam. This observation could be due to the long range of more energetic electrons generated in the beam proximal to the implant.

The range of backscattered electrons is relatively short. As displayed in table 1, the DCFs fall off quickly with distance from the nylon-prosthesis proximal interface. For instance, for the (10 × 10) cm^2 field it changes from 1.21 at 0.1 cm from the interface to 1.11 at 0.5 cm. The trend shown in table 1 has also been reported elsewhere [2,7,16]. The relatively short range of backscattered electrons suggests that the energy of backscattered electrons is rather low [16].

The perturbation effects of prostheses are well reported in literature, though with variations from one study to the other. Also, most reports are restricted to photon attenuation on the transmission side of the implant. For a Ti alloy attenuations which ranged from 0.26-0.28 and 0.17-0.20 at a depth of 10 cm in a water phantom were reported by Sibata et al. [8] for (15 × 15) cm^2 6 MV and 18 MV photon beams, respectively. The results presented in this study indicate that the dose enhancement on the proximal side of the prosthesis shows a marginal variation with field size. A slight change of dose increase with field size has also been reported [11,16]. For various materials evaluated in photon beams from 6-24 MV the dose enhancement remained constant with field size between (4 × 4) and (20 × 20) cm^2 [16]. The field size independence of the DCF is ascribed to electron transport [16].

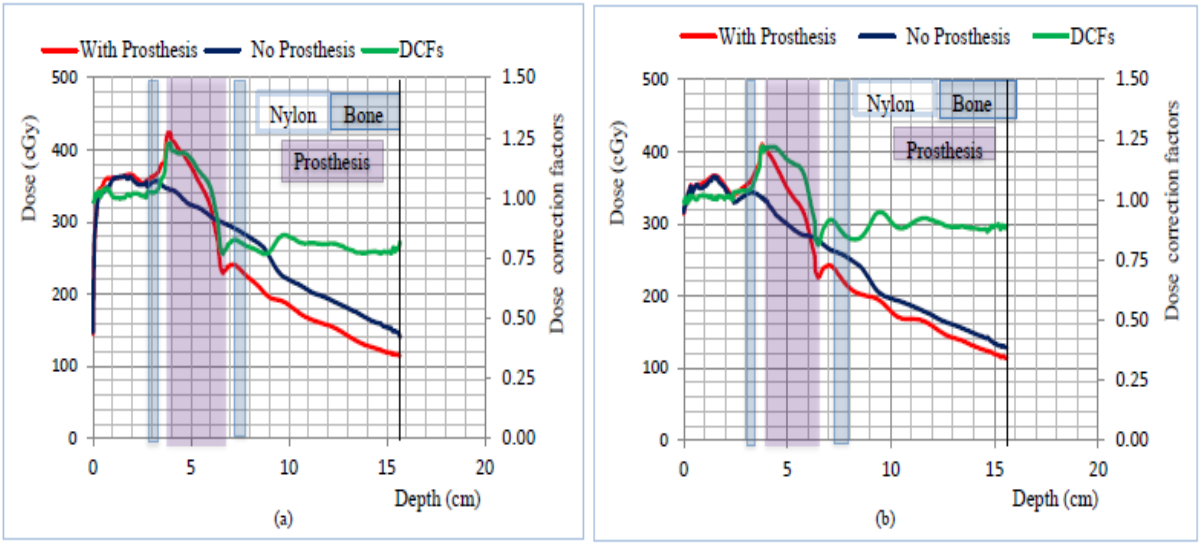

Figure 4: Variation of 6 MV beam depth dose data with and without prosthesis for (a) (5 x 5) cm^2 and (b) (3 x 3) cm^2 fields. Dose correction factors with depth are shown by the green curve.

Table 1. Variation of DCFs with distance from the proximal nylon-prosthesis interface for a range of field sizes.

Distance (cm)	(3 × 3) cm^2	(5 × 5) cm^2	(10 × 10) cm^2
0.1	1.20	1.21	1.21
0.2	1.12	1.19	1.20
0.3	1.09	1.10	1.17
0.5	1.05	1.07	1.11

4. Conclusions

In this study 6 MV photon beam dose perturbations of unilateral Ti prosthesis have been measured in a pelvic prosthesis phantom using Gafchromic EBT2 films. For the studied field sizes, the magnitude of dose enhancement ranged between 22±2% and 23±2% at the nylon-prosthesis interface on the proximal side of the prosthesis. Similarly, dose attenuations between 18±2% and 21±2% were observed in the distal region of the prosthesis. The degree of dose enhancement showed a marginal variation with field size, the dose reduction increased at the (5 × 5) cm^2 field and varied only slightly for the (3 × 3) and (10 × 10) cm^2 fields. DCFs were found to drop off with distance from the proximal interface of the prosthesis. The presentation suggests that significant alteration in absorbed dose distribution by hip prosthesis during radiation therapy could affect clinical outcome.

Acknowledgements

This research and the publication thereof is the result of funding provided by the Medical Research Council of South Africa in terms of the MRC's Flagships Awards Project SAMRC- RFA-UFSP-01-2013/HARD.

References

[1] Wieslander E and Knöös T 2003 *Phys. Med. Biol.* **48** 3295.
[2] Reft C, Alecu R, Das IJ, Gerbi BJ, Keall P, Lief E, Mijnheer BJ, Papanikolaou N, Sibata C and Van Dyk J 2003 *Med Phys*. **30** 1162.
[3] Spezi E, Palleri F, Angelini A L, Ferri A and Baruffaldi F 2007 *J Phys Conf Ser*. **74** 021016.
[4] Carolan M, Dao P, Fox C and Metcalfe P 2000 *Australas Radiol*. **44** 290.
[5] Keall PJ, Siebers J V, Jeraj R and Mohan R 2003 *Med Dosim*. **28** 107.
[6] Fattahi S and Ostapiak OZ 2012 *J Appl Clin Med Phys*. **13** 3347.
[7] Mesbahi A and Nejad FS 2007 *Radiat Med – Med Imaging Radiat Oncol*. **25** 529.
[8] Sibata CH, Mota HC, Higgins PD, Gaisser D, Saxton JP and Shin KH 1990 *Int J Radiat Oncol Biol Phys*. **18** 455.
[9] Chatzigiannis C, Lymperopoulou G, Sandilos P, Dardoufas C, Yakoumakis E, Georgiou E and Karaiskos E 2011 *J Appl Clin Med Phys*. **12** 3295.
[10] Erlanson M and Franzén L 1991 *Int J Radiat Oncol. Biol Phys*. **20** 1093.
[11] Biggs PJ and Russell MD 1998 *Int J Radiat Oncol Biol Phys*. **14** 581.
[12] Jones AK, Hintenlang DE and Bolch WE 2003. *Med Phys*. **30** 2072.
[13] Fuss M, Sturtewagen E, De Wagter C and Georg D 2007 *Phys Med Biol*. **52** 4211.
[14] Lewis D, Micke A, Yu X and Chan MF 2012 *Med Phys*. **39** 6339.
[15] Ding GX and Yu CW 2001 *Int J Radiat Oncol Biol Phys*. 5**1** 1167.
[16] Das IJ and Kahn FM 1997 *Med Phys*.**16** 367.